Received: 1 February 2022 | Revised: 12 April 2022 | Accepted: 13 May 2022

DOI: 10.1002/prca.202200015

Proteomics Clinical Applications

RESEARCH ARTICLE

Proteomic profiling of idiopathic Parkinson's disease primary patient cells by SWATH-MS

Stephen A. Wood[1] | Peter G. Hains[2] | Arnaud Muller[3] | Melissa Hill[1] | Susitha Premarathne[1] | Mariyam Murtaza[1] | Phillip J. Robinson[2] | George D. Mellick[1] | Alex M. Sykes[1]

[1]Griffith Institute for Drug Discovery, Griffith University, Nathan, Queensland, Australia

[2]Cell Signalling Unit, Children's Medical Research Institute, The University of Sydney, Westmead, NSW, Australia

[3]Luxembourg Institute of Health, Dudelange, Luxembourg

Correspondence
Alex M. Sykes, Griffith Institute for Drug Discovery, Griffith University, Nathan, Queensland 4111, Australia.
Email: a.sykes@griffith.edu.au

Abstract

Purpose: Parkinson's disease (PD) is the second most prevalent neurodegenerative disease. It is generally diagnosed clinically after the irreversible loss of dopaminergic neurons and no general biomarkers currently exist. To gain insight into the underlying cellular causes of PD we aimed to quantify the proteomic differences between healthy control and PD patient cells.

Experimental Design: Sequential Window Acquisition of all THeoretical Mass Spectra was performed on primary cells from healthy controls and PD patients.

Results: In total, 1948 proteins were quantified and 228 proteins were significantly differentially expressed in PD patient cells. In PD patient cells, we identified seven significantly increased proteins involved in the unfolded protein response (UPR) and focused on cells with high and low amounts of PDIA6 and HYOU1. We discovered that PD patients with high amounts of PDIA6 and HYOU1 proteins were more sensitive to endoplasmic reticulum stress, in particular to tunicamycin. Data is available via ProteomeXchange with identifier PXD030723.

Conclusions and Clinical Relevance: This data from primary patient cells has uncovered a critical role of the UPR in patients with PD and may provide insight to the underlying cellular dysfunctions in these patients.

KEYWORDS
Parkinson's disease, proteomics

1 | INTRODUCTION

Parkinson's disease (PD) is a neurodegenerative disease affecting 1% of people over 60%, and 3% of those over 80 [1, 2]. PD is diagnosed primarily on the presence of motor symptoms including bradykinesia, resting tremor, rigidity and postural instability. These motor symptoms arise due to the slow, progressive loss of dopaminergic (DA) neurons in the substantia nigra pars compacta (SNpc) in the midbrain [2]. The precise aetiology of disease in 90% of PD patients (idiopathic PD [iPD]) is unknown, attributed to complex interactions between multiple genetic variations and exposure to environmental stresses unique to each patient [3, 4].

Dysfunction in a number of cellular organelles has been implicated in PD pathology, including mitochondria, endo-lysosomes and

Abbreviations: PD, Parkinson's disease; iPD, Idiopathic Parkinson's disease; ER, endoplasmic reticulum; ONS, olfactory neuroepithelial derived cells; qRT-PCR, quantitative reverese transcription PCR; UPR, unfolded protein response; GO, Gene Ontology; 6-OHDA, 6-hydroxydopamine; MPP+, 1-methyl-4-phenylpyridinium.

proteasomes [2]. Despite this seemingly daunting heterogeneity and complexity of PD pathogenesis, it is clear that PD manifests in general on a background of increased ageing [2]. In addition, while the molecular mechanism initiating disease and the subsequent additive insults, both genetic and environmental, are unknown, the final common cellular phenotype is the presence of large intracellular aggregates called Lewy bodies, comprised predominantly of misfolded α-synuclein protein [2, 3, 5]. This shared endpoint, arrived at after decades of incremental accumulation of cell dysfunctions in post-mitotic DA neurons, has led to the hypothesis that reduced buffering capacity of proteostasis networks is a major contributing factor to PD [6, 7]. Not surprisingly, multiple cellular mechanisms including the endoplasmic reticulum (ER) proteasomes, lysosomes and autophagy are dedicated to maintaining protein balance [6–9].

In this study, we performed Sequential Window Acquisition of all THeoretical Mass Spectra (SWATH-MS) on primary patient olfactory neuroepithelial derived cells (ONS) from both iPD and healthy controls and identified 228 differentially quantified proteins. Reactome pathway analysis revealed that the 'Neutrophil degranulation and XBP1(S) activate chaperone genes pathways' were the most affected, indicating disruption of the secretory pathway. Upon closer inspection we identified that proteins associated with the ER and the secretory pathways were the most abundantly changed, in particular proteins associated with the unfolded protein response (UPR). In order to validate this finding, we performed qRT-PCR analysis on patient ONS subjected to ER stressors and confirmed that the iPD patient cells had elevated UPR responses, in particular to tunicamycin mediated ER stress.

2 | MATERIALS AND METHODS

2.1 | Ethics statement

All donor tissue and information were obtained with informed and written consent of the participants. All procedures were in accordance with National Health and Medical Research Council Code of Practice for Human Experimentation and approved by the Griffith University Human Experimentation Ethics Committee.

2.2 | Patient derived ONS cells

Olfactory neuroepithelium-derived cells (ONS) derived from patients with iPD or from healthy control subjects were established as previously described [10]. No information regarding disease severity was recorded.

2.3 | Cell culture

ONS cells were cultured in DMEM/F12 (Thermo Fisher Scientific) supplemented with 10% foetal bovine serum (Thermo Fisher Scientific). For proteomics, cells were grown until confluence in a T75 flask (Nunc) then scraped, pelleted and stored at −80°C until analysed. For qRT-PCR experiments cells were grown until confluence in six well plates (Nunc) before treatment with Tunicamycin (Sigma), Brefeldin A (BFA, Merck) or Thapsigargin (Sigma).

2.4 | Cell line lysis and digestion

Cell line pellets were resuspended in 500 μl 8 M urea, 50 mM NH_4HCO_3, pH 7.8 and sonicated on ice for 10 s (Branson Sonifier 150). The lysate was centrifuged for 20 min, 18,000 *g*, 4°C and the protein content of the supernatant determined using a BCA assay. Lysate (500 μg) was then reduced (4 mM DTT), 30 min at 21°C to avoid carbamylation due to urea and alkylated (12 mM iodoacetamide), 50 min at 21°C in the dark.

Samples were digested with Lys-C (Wako) for 4 h at room temperature. Next, they were diluted with 50 mM NH_4HCO_3, pH 7.8 to give a concentration of 1 M urea, trypsin (Promega) was added and digestion performed overnight at 21°C. Samples were subjected to SPE using 1 ml 3 M Empore C18 SPE cartridges, lysophilised and resuspended in 0.5% v/v formic acid.

2.5 | MS conditions, IDA

Samples were analysed by mass spectrometry on a Sciex 6600 TripleTOF MS equipped with a Turbo V source and coupled to an Eksigent LC system, loading 4 μg per run. Buffer A was 0.1% v/v formic acid in water. The following gradient was used; 2% buffer B (0.1% v/v formic acid, 99.5% v/v acetonitrile) for 2 min, 2%–10% buffer B over 4 min, 10%–25% buffer B over 60 min, 25%–40% buffer B over 5 min, 40%–95% buffer B over 4 min, 95%–98% buffer B over 5 min, 98%–2% buffer B over 3 min, hold for 13 min, for a total run time of 95 min. Samples were first trapped (SGE 10 mm × 300 μm, C18P), then separated (Dr. Maisch 200 mm × 300 μm, Reprosil Pur basic, 3 μm, 100 Å) at a flow rate of 5 μl/min. Retention time standard peptides were added to all samples prior to LC-MS.

Pools of both PD or control samples made and used to produce a Spectral Reference Library (SRL) using IDA acquisition with MS1 scanning from 350 to 1250 *m/z* for 200 ms and MS2 from 100 to 1500 *m/z* for 50 ms. The top 30 precursors were selected for MS/MS acquisition. Data was searched using ProteinPilot (5.0.1) against Uniprot *Homo sapiens* (10 August 2016, 178,750 proteins, SWISS-PROT and TREMBL) that had the retention standard sequences added. Search parameters were; Sample type: Identification, iodoacetmaide alkylation, tryptic digestion Special factors: urea denaturation, Instrument: TripleTOF 6600, Search effort; Thorough, perform FDR analysis (1% error level used). An SRL of 2792 proteins and 23,191 peptides was used for SWATH analysis. Canonical tryptic peptides made up 78.5% of the peptides observed, Cys was fully converted to Cys-CAM (3740 peptides), carbamylation of K was at 0.2% (24 peptides) and carbamy-

lation of the N-terminus at 1.7% (362 peptides). This data was input into SWATHTuner [11] and 100 variable windows used for SWATH acquisition.

The same LC-MS system was used for SWATH analysis with an identical gradient. MS1 was acquired from 345 to 1500 *m/z* for 150 ms and each MS2 window was acquired for 32 ms from 100 to 1500 *m/z*, high sensitivity acquisition. Each sample was run twice in a randomised fashion. Data was analysed using PeakView (2.2.0.11391) and MS/MS (ALL) with SWATH (2.0.0.2003) with the following settings; 20 peptides per protein, six transitions per peptide, 99% peptide confidence, 1% FDR, exclude modified peptides, use 8 min RT window and 75 ppm width. Data was output from PeakView in the form of a spreadsheet for further analysis.

The mass spectrometry proteomics data have been deposited to the ProteomeXchange Consortium via the PRIDE partner repository [12] with the dataset identifier PXD030723.

2.6 | Data analysis

The FDR threshold was set at 1% at the peptide level, with normalisation at the peptide level using Normalyzer [13] , LOESS normalisation was used for the analysis. Peptides were rolled up using InfernoRDN [14] and the R-rollup function. An ANOVA was performed with InfernoRDN and multiple-test correction performed with SGoF+ [15] .

2.7 | Proteomic result summary

The MS data was searched against the SWISS-PROT and TREMBL human databases (August 2016, 178,750 proteins). A total of 1948 proteins were quantified using SWATH-MS 1505 with two or more peptides. There were 228 proteins with significantly (ANOVA test) different levels when PD and controls were compared for proteins quantified with two, or more, peptides.

2.8 | Functional analysis of proteomics data

Protein features have been considered as significant when the pValue (SGoF) was below 0.05, and amongst the 1950 features, 219 reach such threshold. Next, the experimental protein identifiers which were in the form of a combination of Uniprot (SWISS-PROT and TREMBL) accession number were converted into HGNC Human Gene Symbol using the *R* package biomaRt [16]. The resulting gene symbol list has been submitted to Reactome [17] and GeneOntology [18]. Cellular component databases using clusterProfiler [19] package with the default parameters in order to detect significant function enrichment. The *p*-values were calculated based the hypergeometric model (Boyle et al. 2004) and were adjusted for multiple comparison.

2.9 | cDNA synthesis

RNA was extracted using 500 μl of Trizol (Thermo Fisher Scientific) per well and isolated according to manufacturer's protocols. RNA yield and purity were assessed via NanoDrop (ND-1000). cDNA was synthesised using 1 μg RNA and a High Capacity cDNA Reverse Transcription Kit (Applied Biosystems) according to manufacturer's conditions. cDNA was stored at −20°C until used for qRT-PCR.

2.10 | qRT-PCR

A 1:10 dilution of synthesised cDNA (~2 ng/μl) was used for qRT-PCR analysis. All qRT-PCR reactions were carried out using the commercial PowerUp SYBR Green Master Mix (Applied Biosystems) in a 384-well reaction plate (Micro-Amp EnduraPlate Optical 384-well Clear Reaction Plate, Applied Biosystems). Primers were then applied at a final concentration of 5 μM to a final reaction volume of 10 μl. Primers used: XBP1s F-CTGAGTCCGCAGCAGGTG and R-GTCCAGAATGCCCAACAGGA; BiP F-CATCACGCCGTCCTATGTCG and R-CGTCAAAGACCGTGTTCTCG; GRP94 F-CATTAAGCTCTATG TGCGCCG and R-AGTCTCGCGGGAAACATTCA; TBP1 F-CCACTCA CAGACTCTCACAAC and R-CTGCGGTACAATCCCAGAACT. Plates were sealed (Optical Adhesive Covers, Applied Biosystems) then centrifuged at 500 rcf for 5 min. QuantStudio 6 Flex Real-Time PCR system (Applied Biosystems) was used for all reactions. Cycle conditions were identical for all plates analysed and were as follows: 2 min at 50°C then 2 min at 95°C followed by 40 cycles of 15 s at 95°C, and 1 min at 60°C. Melt curves were generated after each run to confirm single PCR product. All reactions were performed in triplicate and in each run an internal standard curve was generated to assign relative concentrations to the amplicons. Florescence data was converted into cycle threshold measurement using QuantStudio Real-Time PCR Software v1.7.1 (Applied Biosystems).

3 | RESULTS

3.1 | SWATH-MS analysis identifies ER proteins upregulated in iPD ONS

We aimed to investigate whether there were differences in the abundance of proteins between healthy control and iPD patient ONS cells under steady-state conditions in order to gain cellular insights into the underlying differences in iPD patients. ONS cells are obtained from the nasal mucosa and represent cellular deficits between controls and iPD [10, 20, 21] in addition to being α-synuclein naïve. Thus, investigating PD in these cells could reveal a general, systemic underlying issue in the patients. To this end, we performed SWATH-MS on 16 individual control and 16 individual iPD ONS cells (Table 1).

A total of 1948 proteins were quantified (Table S1) and these results revealed 228 differentially quantified proteins in iPD ONS, 125

TABLE 1 Parkinson's disease patient cohort

	Age (years)		Gender**	
	Range	Mean*	Female	Male
Control	27–64	52.75 ± 10.5	10	6
PD	34–79	59.87 ± 10.2	6	10

Proteomics analysis was performed to investigate the molecular mechanisms underpinning the functional differences between PD-derived and control ONS cell lines. Protein was collected from early passage ONS cell lines derived from 16 idiopathic PD patients (six female; 10 male; age 59.87 ± 10.2 years) and 16 healthy controls (10 female; six male; 52.75 ± 10.5 years) under normal culture conditions. No significant differences were found in age (*$p = 0.07$) or gender (**$p = 0.157$) between control and PD patients. PD, Parkinson's disease; ONS, olfactory neuroepithelial derived cells.

increased and 103 decreased (Figure 1A). Of the known PD associated proteins, only DJ-1 and VPS35 were detected by SWATH-MS. However, both were significantly reduced in the iPD ONS. In support for ONS cells being α-synuclein naïve we did not detect α-synuclein peptides and ONS cells are also negative by qRT-PCR (Hill and Sykes unpublished data). As the iPD ONS cells were isolated from patients with no known genetic causes of PD we first sought to understand how these differentially represented proteins may be connected. To do this, we performed Reactome pathway enrichment analysis on the differentially represented proteins and observed 42 significantly differentially represented pathways. The 'neutrophil degranulation', 'signalling by receptor tyrosine kinases', 'platelet activation', 'signalling and aggregation' and 'translation' pathways had the highest gene ratio representation (Figure 1B, C). The majority of the pathways altered in iPD ONS cells were involved in post-Golgi signalling pathways. Interestingly, upon closer inspection we discovered that 8/42 pathways were directly linked to the ER and ER proteostasis. Together these data suggest a general underlying deficit in the secretory pathway of iPD patients.

To gain further insight into the protein differences between control and iPD cells we next performed Gene Ontology (GO) term enrichment analysis (Figure 2A). This analysis revealed that the most significant GO terms were associated with secretion, the ER, apoptosis and cell signalling. Upon closer inspection, as with the reactome analysis, we identified that proteins associated with the ER and the secretory pathways were the most abundantly changed, in particular proteins associated with the UPR. These proteins included protein transport protein Sec61 subunit alpha isoform 1 (SEC61A1), protein transport protein Sec61 subunit beta (SEC61bEC6V-type proton ATPase subunit d 1 (V-ATPase D), signal recognition particle receptor subunit alpha (SRPRA), signal recognition particle receptor subunit beta (SRPRB), protein disulphide-isomerase A6 (PDIA6) and hypoxia upregulated protein 1 (HYOU1) (Figure 2B).

In summary, unmanipulated iPD ONS cells have altered levels of proteins primarily involved in secretion, in particular ER proteins involved in the UPR. In iPD ONS cells, the dysregulation of integral ER and secretory proteins may represent an underlying cellular dysfunction that is exacerbated under certain genetic and/or environmental stressors, precipitating PD symptoms later in life.

3.2 | PDIA6/HYOU1 high iPD cells have enhanced UPR responses

Even though there are some known genetic factors causes of early onset of Parkinsonism, primarily involving genes directly associated with mitochondrial dysfunction (parkin and PINK-1 mutations [22]), PD is commonly diagnosed in patients over 50 years of age. As such, patients with PD generally live without obvious symptoms for many years. We discovered that iPD cells had elevated UPR related proteins at basal conditions, therefore we sought to determine if this increase in UPR proteins was related to a functional deficit, that is increased sensitivity to ER stress. To test this, we selected cell lines based on their PDIA6/HYOU1 protein levels, which are directly regulated by the UPR, and assessed the UPR after stress. To this end, we selected six control (PDIA6/HYOU1^{low}) and six iPD (PDIA6/HYOU1^{high}) cell lines and investigated their UPR response after induction using tunicamycin (1 μg/ml), a commonly used ER stressor [23, 24]. First, we established the optimum time after incubation for UPR induction by treating 6 pooled ONS cells with tunicamycin over an 8-h period. In these experiments, we observed UPR induction 6 h post-tunicamycin treatment and the highest response 8 h after treatment (Figure 3). Thus, we chose 8 h post-stressor for downstream experiments. As tunicamycin inhibits the first step of glycosylation, resulting in accumulation of misfolded proteins in the lumen of the ER [23], we also induced the UPR by BFA, which inhibits COP-I vesicle transport from the ER to the Golgi [25] and results in accumulation of correctly folded proteins en route to the Golgi apparatus [26, 27]. As expected, when we measured UPR responsive transcripts (XBP1s, CHOP and BiP) in untreated cells, we observed low relative expression levels in control cells (0.0034 ± 0.0024, 0.0147 ± 0.0091, 0.0065 ± 0.0028, respectively) (Figure 4A–C). Interestingly, we observed higher relative expression levels in iPD cells (0.0061 ± 0.0025, 0.0463 ± 0.0262, 0.0181 ± 0.0123, respectively) (Figure 4A–C). Strikingly, when UPR was induced by tunicamycin for 8 h we discovered that iPD cells had significantly increased expression of all measured UPR transcripts (Figure 4D–F). When UPR was induced by BFA, only XBP1s was significantly increased and both the CHOP and BiP transcripts were unchanged between control and iPD ONS indicating that the iPD (PDIA6/HYOU1^{high}) cells are more sensitive to misfolded protein induced ER stress (Figure 4G–I).

4 | DISCUSSION

In this study, we identified by SWATH-MS differentially quantified proteins between control and iPD ONS. Reactome and GO analysis identified secretory pathways as being the most represented, in particular proteins involved in the UPR. We next focused on the ER/UPR pathways due to their importance in PD pathogenesis [28, 29] and discovered that an abundance of ER proteins and UPR related proteins

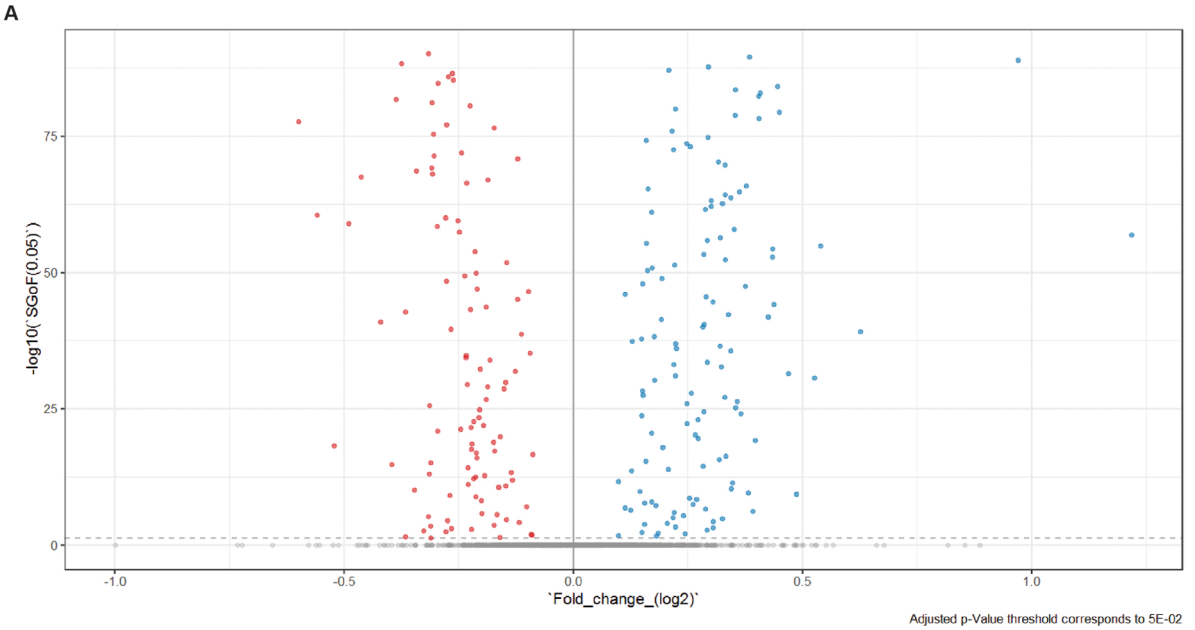

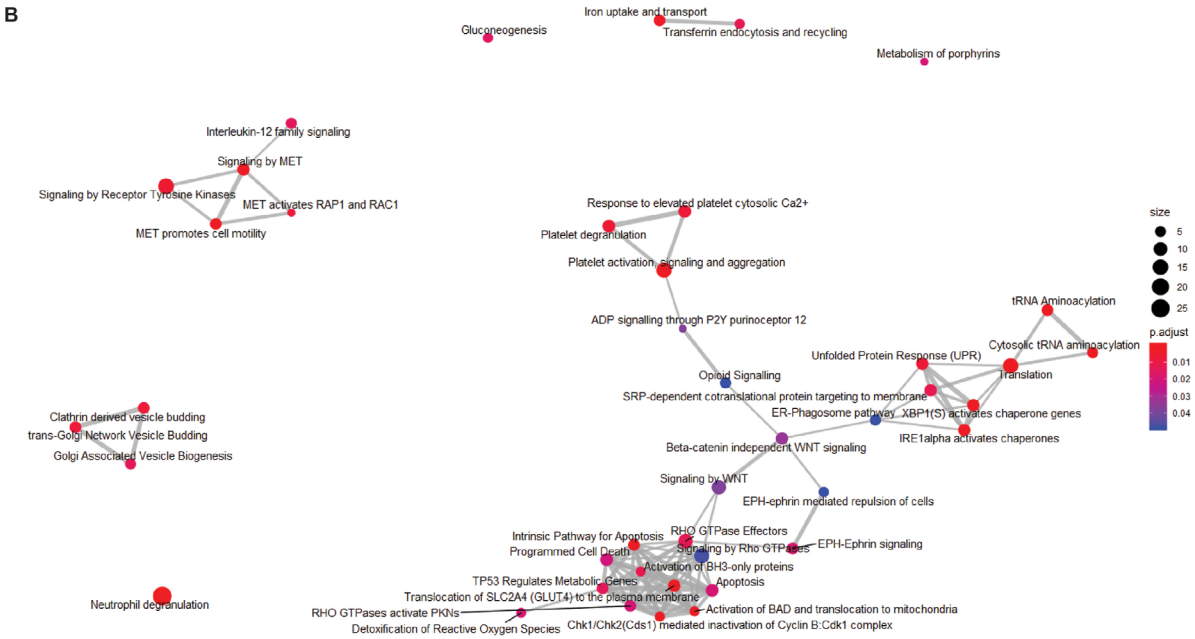

C

ID	Description	GeneRatio	BgRatio	p.adjust
R-HSA-6798695	Neutrophil degranulation	27/130	479/10554	1.19e-08
R-HSA-76002	Platelet activation, signaling and aggregation	14/130	262/10554	0.000869
R-HSA-381038	XBP1(S) activates chaperone genes	7/130	57/10554	0.000869
R-HSA-381070	IRE1alpha activates chaperones	7/130	59/10554	0.000869
R-HSA-379716	Cytosolic tRNA aminoacylation	5/130	24/10554	0.000869
R-HSA-8875878	MET promotes cell motility	6/130	41/10554	0.000869
R-HSA-379724	tRNA Aminoacylation	6/130	42/10554	0.000869
R-HSA-72766	Translation	14/130	291/10554	0.000869
R-HSA-75035	Chk1/Chk2(Cds1) mediated inactivation of Cyclin B:Cdk1 complex	4/130	13/10554	0.000869
R-HSA-109606	Intrinsic Pathway for Apoptosis	6/130	44/10554	0.000869

FIGURE 1 iPD patients have a dysregulation of proteins in the secretory pathway. (A) Volcano plot of proteins which are differentially represented in iPD ONS. Red corresponds to 103 significantly decreased and blue 125 significantly increased proteins. (B) AReactome network sorted by *p* value. (C) Table of the top 10 most significant altered reactome pathways. iPD, idiopathic Parkinson's disease; ONS, olfactory neuroepithelial derived cells

A

ID	Description	GeneRatio	BgRatio	p.adjust
GO:1904813	ficolin-1-rich granule lumen	12/154	249/30786	8.66e-07
GO:0101002	ficolin-1-rich granule	15/154	364/30786	1.71e-07
GO:0042470	melanosome	10/154	215/30786	1.19e-05
GO:0048770	pigment granule	10/154	215/30786	1.19e-05
GO:0030117	membrane coat	5/154	196/30786	0.0445
GO:0048475	coated membrane	5/154	196/30786	0.0445
GO:0008250	oligosaccharyltransferase complex	2/154	17/30786	0.0445
GO:0031234	extrinsic component of cytoplasmic side of plasma membrane	5/154	184/30786	0.0377
GO:0001726	ruffle	7/154	338/30786	0.0312
GO:0098562	cytoplasmic side of membrane	7/154	341/30786	0.0312
GO:0044309	neuron spine	7/154	345/30786	0.0312
GO:0030118	clathrin coat	4/154	104/30786	0.0312
GO:0030666	endocytic vesicle membrane	7/154	332/30786	0.0304
GO:0071782	endoplasmic reticulum tubular network	3/154	43/30786	0.029
GO:0005905	clathrin-coated pit	5/154	151/30786	0.0237
GO:0005766	primary lysosome	7/154	293/30786	0.0182
GO:0042582	azurophil granule	7/154	293/30786	0.0182
GO:0031258	lamellipodium membrane	3/154	33/30786	0.0181
GO:0005790	smooth endoplasmic reticulum	4/154	69/30786	0.0134
GO:0019897	extrinsic component of plasma membrane	8/154	329/30786	0.00975
GO:0030027	lamellipodium	9/154	387/30786	0.00633
GO:0030867	rough endoplasmic reticulum membrane	4/154	49/30786	0.00508
GO:0043209	myelin sheath	9/154	329/30786	0.00246
GO:0005791	rough endoplasmic reticulum	7/154	163/30786	0.00126

B

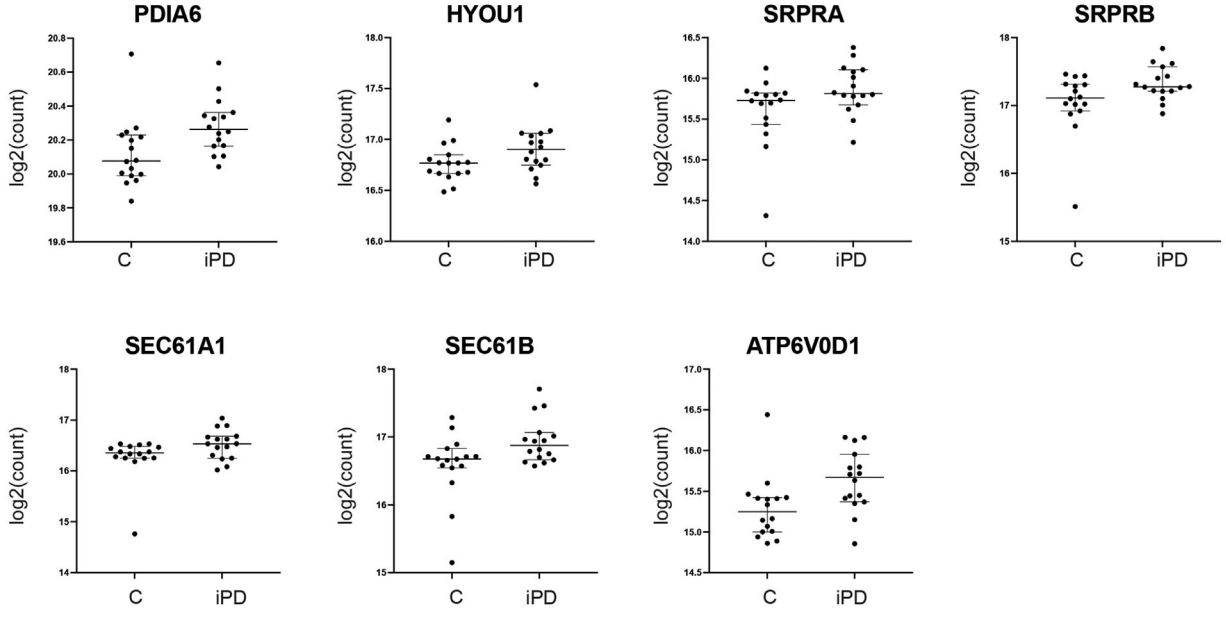

FIGURE 2 iPD patients have a dysregulation of UPR related proteins. (A) GO table, sorted by *p* value of pathways significantly altered in iPD ONS. (B) Scatter plots of the significantly upregulated UPR related proteins in iPD ONS. Data points represent the log2 peptide count from individual cells, lines represent the median and error bars the 95% confidence interval. GO, Gene Ontology; iPD, idiopathic Parkinson's disease; ONS, olfactory neuroepithelial derived cells; UPR, unfolded protein response

were significantly increased in a proportion of the iPD patient cells. We validated the importance of this increase in ER chaperones by developing a functional qRT-PCR assay using ER stress inducers and uncovered that iPD (PDIA6/HYOU1^{high}) ONS cells are more responsive to UPR stress than healthy (PDIA6/HYOU1^{low}) control ONS cells, in particular unfolded protein stress.

Of the 228 differentially represented proteins only 11 were associated with the mitochondria, suggesting that mitochondrial deficits are not the primary cause of functional differences observed in the ONS cell model of iPD [10, 20, 30] in comparison to monogenic PD which have strong mitochondrial deficits (e.g. *PRKN*, *PINK1* and *PARK7*) [31]. Moreover, of the known 21 proteins associated with PD [32] only

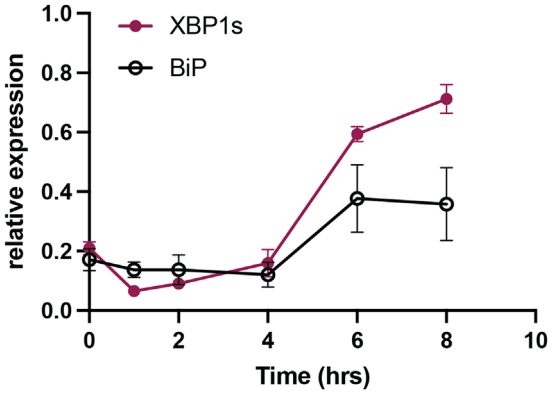

FIGURE 3 Tunicamycin effectively induces the UPR in ONS. qRT-PCR analysis revealed that 8 h after treatment with tunicamycin (1 μg/ml) was the peak expression levels of both XBP1s and BiP. Data represent the mean ± SEM ($n = 3$, six pooled ONS cells). ONS, olfactory neuroepithelial derived cells; UPR, unfolded protein response

VSP35 and DJ-1 were differentially represented, both significantly reduced in the iPD cells. Decreased mRNA and protein levels of DJ-1 are associated with neurodegeneration [33] and may contribute to the iPD patient disease. Furthermore, VPS29 and sorting nexin-1, which are two key components of the reteromer complex along with VPS35, were also significantly decreased in iPD patients. As the reteromer complex is crucial for endosome sorting, it further suggests that these iPD patients have impairments in the endo-lysosomal pathway.

In this study, the most abundantly represented pathways, differentiating PD and control cells by both Reactome and GO analysis were directly related to the secretory protein process: from the ER, the Golgi and vesicular trafficking. This was unexpected as the mitochondria dysfunction is recognised as an important factor in PD [34]. Indeed, it has more recently been identified that ER stress [35] and the endo-lysosomal [36] pathways are affected in PD models using α-synuclein mediated toxicity. Furthermore, rotenone, MPP+ and 6-OHDA, commonly used stressors in laboratory models for PD, also induce ER stress in neuronal cells [28]. Based on these data we hypothesise that iPD cells have general protein quality control and secretion deficits. These deficits may contribute to α-synuclein pathology in the dopaminergic neurons of the SNpc as well as many other cell types which contribute to the myriad of PD symptoms.

Our finding that iPD ONS has increased levels of UPR proteins when cells are grown under basal conditions also indicates an underlying cellular dysfunction. In neurodegenerative diseases, including Parkinson's, there have been reports of increased UPR proteins associated with disease affected patients and in laboratory models of the disease

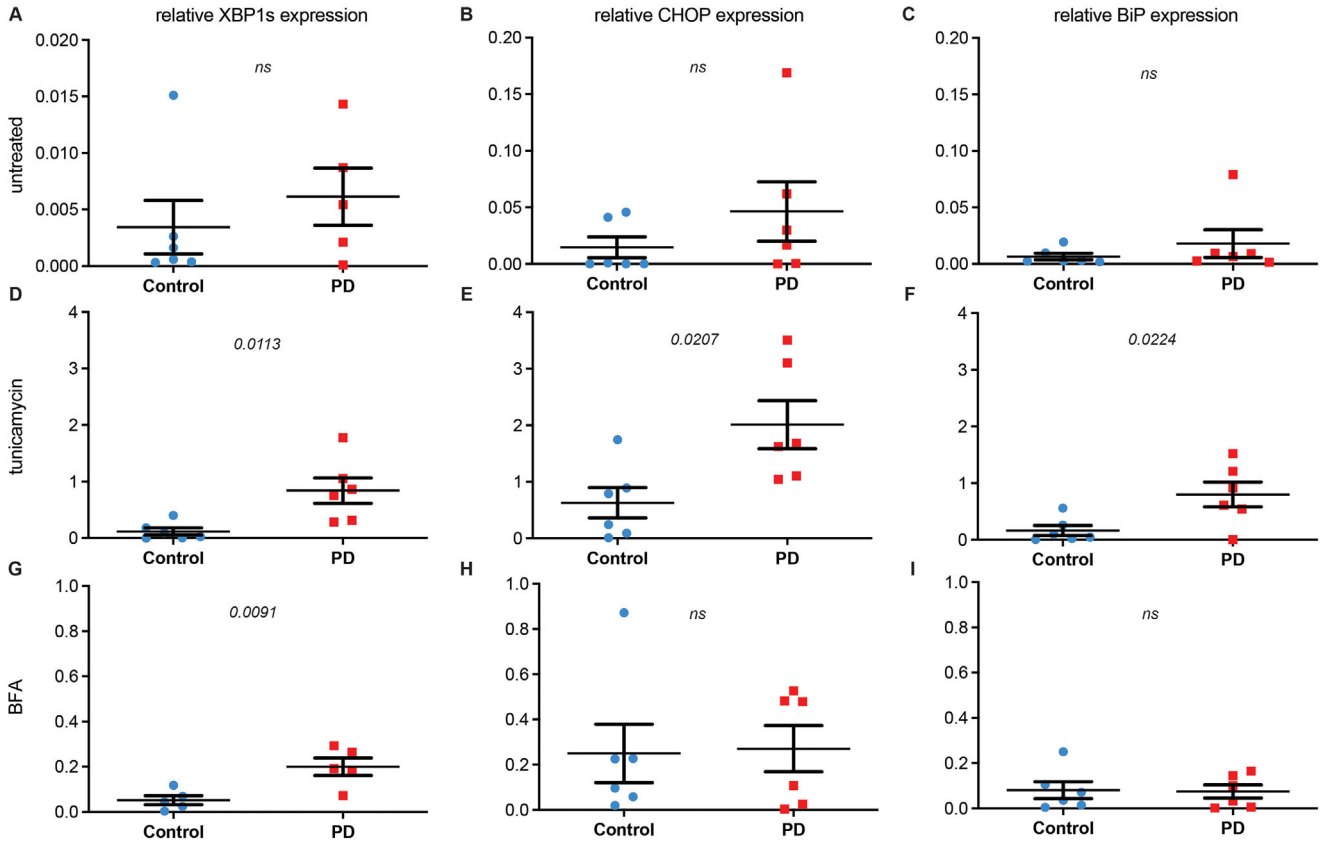

FIGURE 4 Tunicamycin induces an enhanced UPR response in iPD cells. qRT-PCR analysis of XBP1s expression (A, D, G), CHOP expression (B, E, H) and BiP expression (C, F, I) either untreated (A–C), 1 μg/ml tunicamycin for 8 h (D–F) or 1 μg/ml BFA for 8 h (G–I). Data represented as mean ± SEM ($n = 6$ control cell lines or $n = 6$ iPD lines), p values from unpaired t-test. iPD, idiopathic Parkinson's disease; UPR, unfolded protein response

[37, 38]. Importantly the primary patient cell model we have utilised is unperturbed, as we have not used PD associated stressors such as 6-OHDA, MPP+ or rotenone; none-the-less we still observe impaired proteostasis. Furthermore, the ONS cells are α-synuclein naïve so the deficits observed reflect systemic cellular differences. Furthermore, these primary patient cells do have stress specific responses [21] and in the context of this study, cells with high steady-state PDIA6/HYOU1 protein levels have enhanced UPR responses. This could reflect an underlying cellular dysfunction in these patients whereby the basal UPR is upregulated in response to protein quality control and folding issues. ER stress inhibitors such as salubrinal protect against rotenone induced toxicity in SH-SY5Y cells [39]. Likewise, in 3D5 cells and primary neuronal cultures treated with sodium butyrate which induces α-syn oligomerisation, salubrinal treatment increased cell survival and decreased α-syn oligomerisation. Further studies using ER stress inhibitors such as salubrinal on non-α-syn models will be paramount in understanding the cellular dysfunctions in PD patients.

ACKNOWLEDGMENTS

Open access publishing facilitated by Griffith University, as part of the Wiley - Griffith University agreement via the Council of Australian University Librarians.

CONFLICT OF INTEREST

The authors declare they have no conflicts of interest to disclose.

DATA AVAILABILITY STATEMENT

Proteomic data is are freely available via ProteomeXchange with identifier PXD030723.

ORCID

Stephen A. Wood https://orcid.org/0000-0002-2576-7457
Peter G. Hains https://orcid.org/0000-0002-7276-1760
Melissa Hill https://orcid.org/0000-0001-8077-0889
Phillip J. Robinson https://orcid.org/0000-0002-7878-0313
George D. Mellick https://orcid.org/0000-0002-7211-4651
Alex M. Sykes https://orcid.org/0000-0001-8981-6652

REFERENCES

1. Tysnes, O.-B., & Storstein, A. (2017). Epidemiology of Parkinson's disease. *Journal of Neural Transmission*, *124*, 901–905.
2. Kalia, L. V., & Lang, A. E. (2015). Parkinson's disease. *The Lancet*, *386*, 896–912.
3. Antony, P. M. A., Diederich, N. J., Krüger, R., & Balling, R. (2013). The hallmarks of Parkinson's disease. *FEBS Journal*, *280*(23), 5981–93. 10.1111/febs.12335
4. Couteur, D. G. L., Muller, M., Yang, M. C., Mellick, G. D., & Mclean, A. J. (2002). Age-environment and gene-environment interactions in the pathogenesis of Parkinson's disease. *Reviews on Environmental Health*, *17*, 51–64.
5. Riederer, P., Berg, D., Casadei, N., Cheng, F., Classen, J., Dresel, C., Jost, W., Krüger, R., Müller, T., Reichmann, H., Rieß, O., Storch, A., Strobel, S., Van Eimeren, T., Völker, H.-U., Winkler, J., Winklhofer, K. F., Wüllner, U., Zunke, F., & Monoranu, C.-M. (2019). α-Synuclein in Parkinson's disease: Causal or bystander? *Journal of Neural Transmission*, *126*, 815–840.
6. Klaips, C. L., Jayaraj, G. G., & Hartl, F. U. (2018). Pathways of cellular proteostasis in aging and disease. *Journal of Cell Biology*, *217*, 51–63.
7. Lázaro, D. F., & Outeiro, T. F. (2020). The interplay between proteostasis systems and Parkinson's disease. *Advances in Experimental Medicine and Biology*, *1233*, 223–236.
8. Hetz, C., & Saxena, S. (2017). ER stress and the unfolded protein response in neurodegeneration. *Nature Reviews Neurology*, *13*, 477–491.
9. Lin, J. H., Walter, P., & Yen, T. S. B. (2008). Endoplasmic reticulum stress in disease pathogenesis. *Annual Review of Pathology: Mechanisms of Disease*, *3*, 399–425.
10. Matigian, N., Abrahamsen, G., Sutharsan, R., Cook, A. L., Vitale, A. M., Nouwens, A., Bellette, B., An, J., Anderson, M., Beckhouse, A. G., Bennebroek, M., Cecil, R., Chalk, A. M., Cochrane, J., Fan, Y., Féron, F., Mccurdy, R., Mcgrath, J. J., Murrell, W., … Mackay-Sim, A. (2010). Disease-specific, neurosphere-derived cells as models for brain disorders. *DMM Disease Models & Mechanisms*, *3*, 785–798.
11. Zhang, Y., Bilbao, A., Bruderer, T., Luban, J., Strambio-De-Castillia, C., Lisacek, F., Hopfgartner, G., & Varesio, E. (2015). The use of variable Q1 isolation windows improves selectivity in LC–SWATH–MS acquisition. *Journal of Proteome Research*, *14*, 4359–4371.
12. Perez-Riverol, Y., Csordas, A., Bai, J., Bernal-Llinares, M., Hewapathirana, S., Kundu, D. J., Inuganti, A., Griss, J., Mayer, G., Eisenacher, M., Pérez, E., Uszkoreit, J., Pfeuffer, J., Sachsenberg, T., Yılmaz, Ş., Tiwary, S., Cox, J., Audain, E., Walzer, M., … Vizcaíno, J. A. (2019). The PRIDE database and related tools and resources in 2019: Improving support for quantification data. *Nucleic Acids reSearch*, *47*, D442–D450.
13. Chawade, A., Alexandersson, E., & Levander, F. (2014). Normalyzer: A tool for rapid evaluation of normalization methods for omics data sets. *Journal of Proteome Research*, *13*, 3114–3120.
14. Taverner, T., Karpievitch, Y. V., Polpitiya, A. D., Brown, J. N., Dabney, A. R., Anderson, G. A., & Smith, R. D. (2012). DanteR: An extensible R-based tool for quantitative analysis of -omics data. *Bioinformatics*, *28*, 2404–6.
15. Carvajal-Rodriguez, A., & De Uña-Alvarez, J. (2011). Assessing significance in high-throughput experiments by sequential goodness of fit and q-value estimation. *PLoS ONE*, *6*, e24700.
16. Durinck, S., Spellman, P. T., Birney, E., & Huber, W. (2009). Mapping identifiers for the integration of genomic datasets with the R/Bioconductor package biomaRt. *Nature Protocols*, *4*, 1184–1191.
17. Griss, J., Viteri, G., Sidiropoulos, K., Nguyen, V. Y., Fabregat, A., & Hermjakob, H. (2020). ReactomeGSA – efficient multi-omics comparative pathway analysis. *Molecular & Cellular Proteomics*, *19*, 2115–2125.
18. Carbon, S., Douglass, E., Good, B. M., Unni, D. R., Harris, N. L., Mungall, C. J., Basu, S., Chisholm, R. L., Dodson, R. J., Hartline, E., Fey, P., Thomas, P. D., Albou, L.-P., Ebert, D., Kesling, M. J., Mi, H., Muruganujan, A., Huang, X., Mushayahama, T., … Elser, J. (2021). The Gene Ontology resource: Enriching a GOld mine. *Nucleic Acids Research*, *49*, D325–D334.
19. Wu, T., Hu, E., Xu, S., Chen, M., Guo, P., Dai, Z., Feng, T., Zhou, L., Tang, W., Zhan, L., Fu, X., Liu, S., Bo, X., & Yu, G. (2021). clusterProfiler 4.0: A universal enrichment tool for interpreting omics data. *Innovation (New York, NY)*, *2*, 100141.
20. Cook, A. L., Vitale, A. M., Ravishankar, S., Matigian, N., Sutherland, G. T., Shan, J., Sutharsan, R., Perry, C., Silburn, P. A., Mellick, G. D., Whitelaw, M. L., Wells, C. A., Mackay-Sim, A., & Wood, S. A. (2011). NRF2 activation restores disease related metabolic deficiencies in olfactory neurosphere-derived cells from patients with sporadic Parkinson's disease. *PLoS ONE*, *6*, e21907.
21. Murtaza, M., Shan, J., Matigian, N., Todorovic, M., Cook, A. L., Ravishankar, S., Dong, L. F., Neuzil, J., Silburn, P., Mackay-Sim, A., Mellick, G. D., & Wood, S. A. (2016). Rotenone susceptibility phenotype in olfactory derived patient cells as a model of idiopathic Parkinson's disease. *PLoS ONE*, *11*, 1–19.

22. Klein, C., & Westenberger, A. (2012). Genetics of Parkinson's disease. *Cold Spring Harbor Perspectives in Medicine*, *2*(1), a008888.
23. Mcguckin, M. A., Eri, R. D., Das, I., Lourie, R., & Florin, T. H. (2010). ER stress and the unfolded protein response in intestinal inflammation. *American Journal of Physiology – Gastrointestinal and Liver Physiology*, *298*, 820–832.
24. Gupta, S., Samali, A., Fitzgerald, U., & Deegan, S. (2010). Methods for monitoring endoplasmic reticulum stress and the unfolded protein response. *International Journal of Cell Biology*, *2010*, 830307.
25. Helms, J. B, & Rothman, J. E. (1992). Inhibition by brefeldin a of a Golgi membrane enzyme that catalyses exchange of guanine nucleotide bound to ARF. *Nature*, *360*, 352–354.
26. Shinjo, S., Mizotani, Y., Tashiro, E., & Imoto, M. (2013). Comparative analysis of the expression patterns of UPR-target genes caused by upr-inducing compounds. *Bioscience Biotechnology and Biochemistry*, *77*, 729–735.
27. Zhu, X., Huang, L., Gong, J., Shi, C., Wang, Z., Ye, B., Xuan, A., He, X., Long, D., Zhu, X., Ma, N., & Leng, S. (2017). NF-κB pathway link with ER stress-induced autophagy and apoptosis in cervical tumor cells. *Cell Death Discovery*, *3*, 3–10.
28. Ryu, E. J., et al.(2002). *Endoplasmic Reticulum Stress and the Unfolded Protein Response in Cellular Models of Parkinson's Disease*.
29. Cóppola-Segovia, V., Cavarsan, C., Maia, F. G., Ferraz, A. C., Nakao, L. S., Lima, M. M., & Zanata, S. M. (2017). ER stress induced by tunicamycin triggers α-synuclein oligomerization, dopaminergic neurons death and locomotor impairment: A new model of Parkinson's disease. *Molecular Neurobiology*, *54*, 5798–5806.
30. Murtaza, M., Shan, J., Matigian, N., Todorovic, M., Cook, A. L., Ravishankar, S., Dong, L. F., Neuzil, J., Silburn, P., Mackay-Sim, A., Mellick, G. D., & Wood, S. A. (2016). Rotenone susceptibility phenotype in olfactory derived patient cells as a model of idiopathic Parkinson's disease. *PLoS ONE*, *11*, e0154544.
31. Nuytemans, K., Theuns, J., Cruts, M., & Van Broeckhoven, C. (2010). Human mutation MUTATION UPDATE genes: A mutation update. *Human Mutation*, *31*, 763–780.
32. Blauwendraat, C., Nalls, M. A., & Singleton, A. B. (2020). The genetic architecture of Parkinson's disease. *Lancet Neurology*, *19*, 170–178.
33. Kumaran, R., Vandrovcova, J., Luk, C., Sharma, S., Renton, A., Wood, N. W., Hardy, J. A., Lees, A. J., & Bandopadhyay, R. (2009). Differential DJ-1 gene expression in Parkinson's disease. *Neurobiology of Disease*, *36*, 393–400.
34. Malpartida, A. B., Williamson, M., Narendra, D. P., Wade-Martins, R., & Ryan, B. J. (2021). Mitochondrial dysfunction and mitophagy in Parkinson's disease: From mechanism to therapy. *Trends in Biochemical Sciences*, *46*, 329–343.
35. Mou, Z., Yuan, Y.-H., Zhang, Z., Song, L.-K., & Chen, N.-H. (2020). Endoplasmic reticulum stress, an important factor in the development of Parkinson's disease. *Toxicology Letters*, *324*, 20–29.
36. Wallings, R. L., Humble, S. W., Ward, M. E., & Wade-Martins, R. (2019). Lysosomal dysfunction at the centre of Parkinson's disease and frontotemporal dementia/amyotrophic lateral sclerosis. *Trends in Neuroscience (Tins)*, *42*, 899–912.
37. Colla, E., Coune, P., Liu, Y., Pletnikova, O., Troncoso, J. C., Iwatsubo, T., Schneider, B. L., & Lee, M. K. (2012). Endoplasmic reticulum stress is important for the manifestations of α-synucleinopathy in vivo. *Journal of Neuroscience*, *32*, 3306–3320.
38. Hoozemans, J. J. M., Van Haastert, E. S., Eikelenboom, P., De Vos, R. A. I., Rozemuller, J. M., & Scheper, W. (2007). Activation of the unfolded protein response in Parkinson's disease. *Biochemical and Biophysical Research Communications*, *354*, 707–711.
39. Wu, L., Luo, N., Zhao, H.-R., Gao, Q., Lu, J., Pan, Y., Shi, J.-P., Tian, Y.-Y., & Zhang, Y.-D. (2014). Salubrinal protects against rotenone-induced SH-SY5Y cell death via ATF4-parkin pathway. *Brain Research*, *1549*, 52–62.

SUPPORTING INFORMATION

Additional supporting information can be found online in the Supporting Information section at the end of this article.

How to cite this article: Wood, S. A., Hains, P. G., Muller, A., Hill, M., Premarathne, S., Murtaza, M., Robinson, P. J., Mellick, G. D., & Sykes, A. M. (2022). Proteomic profiling of idiopathic Parkinson's disease primary patient cells by SWATH-MS. *PROTEOMICS – Clinical Applications*, *16*, e2200015. https://doi.org/10.1002/prca.202200015